NUMERICAL SIMULATION ON TEMPERATURE IN WOOD CRIB FIRES

by

Yanhong XI[a], Xue DONG[b], and Wanki CHOW[b*]

[a] Department of Civil Engineering, Beijing Jiaotong University, Beijing, China
[b] Research Centre for Fire Engineering, Department of Building Services Engineering, Hong Kong Polytechnic University, Hong Kong, China

Original scientific paper
https://doi.org/10.2298/TSCI180818288X

Temperature from burning wood cribs will be simulated in this paper by sub-grid scale model in fire dynamics simulator. A baseline gas phase uncertainty is determined for simulating wood crib fire spread scenarios. This uncertainty is based on a sensitivity analysis of key input parameters and their subsequent effect on key output variables that are important for fire spread. Effects of different grid systems, computing domains and moisture contents on the predictions were studied first and then used to study the gaseous phase sensitivity. The gaseous phase input variables considered are: Smagorinsky constant, Prandtl number, and Schmidt number. The results show that the predictions for temperature have good agreement with experiment with the values of 0.25, 0.7, 0.4, and 5 for Smagorinsky constant, turbulent Schmidt number, and turbulent Prandtl number, respectively.

Key words: *wood crib fires, CFD, flammability diagram, gaseous phase sensitivity*

Introduction

Many large-scale construction projects were completed in the Far East. Because of their complex structures and supertall height, most buildings are difficult to meet the fire codes [1]. Performance-based design (PBD) was then applied to determine the necessary fire safety provisions. However, in high-cost consultancy projects, the budget of fire safety studies is often low, being another reason for using PBD as discussed in an Asian conference [2]. The CFD has been widely applied in PBD fire safety performance in such projects [3-6].

Wood is one of the oldest building materials in the world [7]. Wood-based materials are still widely used for structural and nonstructural applications today. A wood apartment was even built in Melbourne, Australia [8]. It is important to understand the fire behavior of burning wood. Wood cribs had been used for studying building fires for many years [9-12]. However, how to simulate accurately by CFD is a very important issue. In the existing research literature, it has not been clearly mentioned. One purpose of the present study is to assess the accuracy of the sub-grid scale model in simulating a wood crib fire by CFD. The CFD software fire dynamics simulator (FDS) version 6 is used.

The prediction of burning processes using large eddy simulation (LES) is satisfactory [13, 14] though the Smagorinsky coefficient has to be selected properly. To properly evaluate the reliability of using FDS in simulating wood crib fire, a baseline gas phase uncertainty

* Corresponding author, e-mail: bewkchow@polyu.edu.hk

of FDS is determined. This uncertainty is based on a sensitivity analysis of key input parameters and their subsequent effect on key output variables that are important for fire spread. In addition, parameters affecting solution of the radiation transport equation can be modified in the group *radiation*. A gray gas model is considered because the use of a wide band model is not practical due to computational expenses and soot is considered as the dominant radiant emitter. Based on the experiment, the gaseous phase input variables were adjusted in the FDS simulations to match with the experimental data. The gaseous phase input variables considered are: Smagorinsky constant, C_s, ranging from 0.1 to 0.25, Prandtl number, from 0.2 to 0.9, and Schmidt number, from 0.2 to 0.9. The results show that the predictions for temperature have a qualitatively good agreement with the experiment by using the appropriate gaseous phase variable value. The results of the present study will be useful for justifying the predications by FDS in big construction projects with fire safety provisions determined by PBD design. This is very important in applying fire models for different applications [15].

Kinetic model

A typical chemical expression for wood compound is $C_{3.4}H_{6.2}O_{2.5}$ [16] which is adopted in the FDS model. According to this expression, the chemical reaction involved in combustion is:

$$C_{3.4}H_{6.2}O_{2.5}+3.7(O_2+3.76N_2)\rightarrow 3.4CO_2+3.1H_2O+3.7\times 3.76N_2 \tag{1}$$

For engineering purposes, one-step reaction assumption is used for modeling the pyrolysis with appropriate kinetic parameters [17].

The most commonly adopted assumption is the one-step first-order Arrhenius expression, which describes reaction and utilizes the simple overall kinetics expressions. According to the Arrhenius law, the kinetic parameters of the non-isothermal solid phase reaction can be effectively calculated based on the conversion rate dα/dt [18]:

$$\frac{\mathrm{d}\alpha}{\mathrm{d}t}=kf(\alpha) \tag{2}$$

In which conversion α and k are given:

$$\alpha=\frac{m_0-m_t}{m_0-m_\infty} \tag{3}$$

$$k=A\mathrm{e}^{-E/RT} \tag{4}$$

where $f(\alpha)$ is the reaction model, m_0, m_t, and m_∞ are sample mass at the initial time, time t, and the final moment, respectively, k [s^{-1}] – the reaction rate constant, A [s^{-1}] – the pre-exponential factor, or frequency factor, E [$kJmol^{-1}$] – the activation energy, R – the universal gas constant (= 8.314×10^{-3} kJ/molK), and T [K] – the reaction temperature.

Based on the pyrolysis rate of pine from Atryea [19], $1.26\cdot10^5$ kJ/molK and $5.1\cdot10^{11}$ 1/s are used for E and A in this paper. The activation energy, E, and pre-exponential factor, A, can be input by users in FDS. In order to describe the gas phase combustion reaction, the *simple chemistry* approach [20, 21] is used. Details of the model introduction are given in FDS technical reference guide [20].

For non-isothermal kinetics, the heating rate $\beta = \mathrm{d}T/\mathrm{d}t$ is introduced into the equation:

$$\frac{\mathrm{d}\alpha}{\mathrm{d}T} = \frac{\mathrm{d}\alpha}{\beta \mathrm{d}t} = \frac{kf(\alpha)}{\beta} = \frac{A\mathrm{e}^{-E/\mathrm{R}T} f(\alpha)}{\beta} \tag{5}$$

$$\int_0^{\alpha} \frac{\mathrm{d}\alpha}{f(\alpha)} = \frac{A}{\beta}\int_{T_0}^{T} \mathrm{e}^{-E/\mathrm{R}T} = \mathrm{g}(\alpha) \tag{6}$$

Letting $x = E/\mathrm{R}T$, eq. (6) can be expressed:

$$\mathrm{g}(\alpha) = \frac{AE}{\beta \mathrm{R}}\left(-\frac{\mathrm{e}^x}{x} + \int_0^{\infty} \frac{\mathrm{e}^x}{x}\mathrm{d}x\right) = \frac{AE}{\beta \mathrm{R}} p(x) \tag{7}$$

As seen from eq. (7), the temperature term, $p(x)$, is a complex integral and has no exact analytical solution. Based on eq. (8), the kinetic parameters could be analyzed by the non-isothermal models [22]:

$$\ln\frac{\beta}{T^{1.92}} = \ln\left[\frac{AE}{\mathrm{R}g(\alpha)}\right] - 0.312 - 1.008\frac{E}{\mathrm{R}T} \tag{8}$$

Comparisons using functional analysis

The functional analysis proposed by Peacock *et al.* [23] was used to evaluate the FDS results [24, 25]. As both experimental and simulated data can be described by transient curves, the technique provides a way to quantify the difference between two curves in terms of magnitude and shape.

The parameters considered here are the norm and the cosine. The norm is a measure of the relative difference in magnitude of the two curves. The data points within each curve are described by vectors, summing them up would give a resultant single vector for each curve. The distance between the resultant vectors for the predicted and measured curves represents error. This error can be normalized to provide a relative difference, or norm, between the curves. The cosine describes the angle between the resultant vectors and provides a quantitative measure of curve shape similarity.

The Euclidean norm and cosine are calculated for each of the point-to-point comparison charts according to:

$$\mathrm{Norm} = \frac{|E-m|}{|E|} = \frac{\sqrt{\sum_{i=1}^{n}(E_i - m_i)^2}}{\sqrt{\sum_{i=1}^{n}(E_i)^2}} \tag{9}$$

$$\mathrm{Cosine} = \frac{\langle E, \vec{\mathrm{M}}\rangle}{|E||\vec{\mathrm{M}}|} = \frac{\sum_{i=2}^{n}\frac{(E_i - E_{i-s})(m_i - m_{i-s})}{t_i - t_{i-1}}}{\sqrt{\sum_{i=2}^{n}\frac{(E_i - E_{i-s})^2}{s^2(t_i - t_{i-1})}\sum_{i=2}^{n}\frac{(m_i - m_{i-s})^2}{s^2(t_i - t_{i-1})}}} \tag{10}$$

where E_i and m_i are the i^{th} experimental and simulation values, t_i – the i^{th} time instant, and s – the number of data points to be considered in each time interval. The parameter s would

smooth and provide better estimates of large scale differences. Here, s is taken as 2. This comparison technique helps validate and quantify observations and conclusions that would otherwise rely on visual observation alone. When achieving a good agreement between the two curves based on experiment and simulation, the values of norm should approach 0, and cosine should be close to 1.

Full-scale burning experiments

Full-scale experiments on wood crib fires with pine were carried out in a room in Hong Kong [21]. The room was of length 3.5 m, width 3.5 m and height 2.4 m as shown in fig. 1(a). The positions of the thermocouple trees are shown in fig. 1(b). The wall was constructed of 0.2 m reinforced concrete. There was a door 1.5 m wide and 2 m tall.

In the fire experiments, the wood crib was positioned at the center of the steel tray at a height of 0.376 m. The wood stack was composed of 16 layers of 40 × 40 mm pine wood sticks and the total height was 0.624 m, as shown in fig. 1(b). The 10 mL of heptane located at the corner of the room was used as the ignition source. Note that the total calorific value and weight of wood were 11350 MJ and 850 kg, respectively.

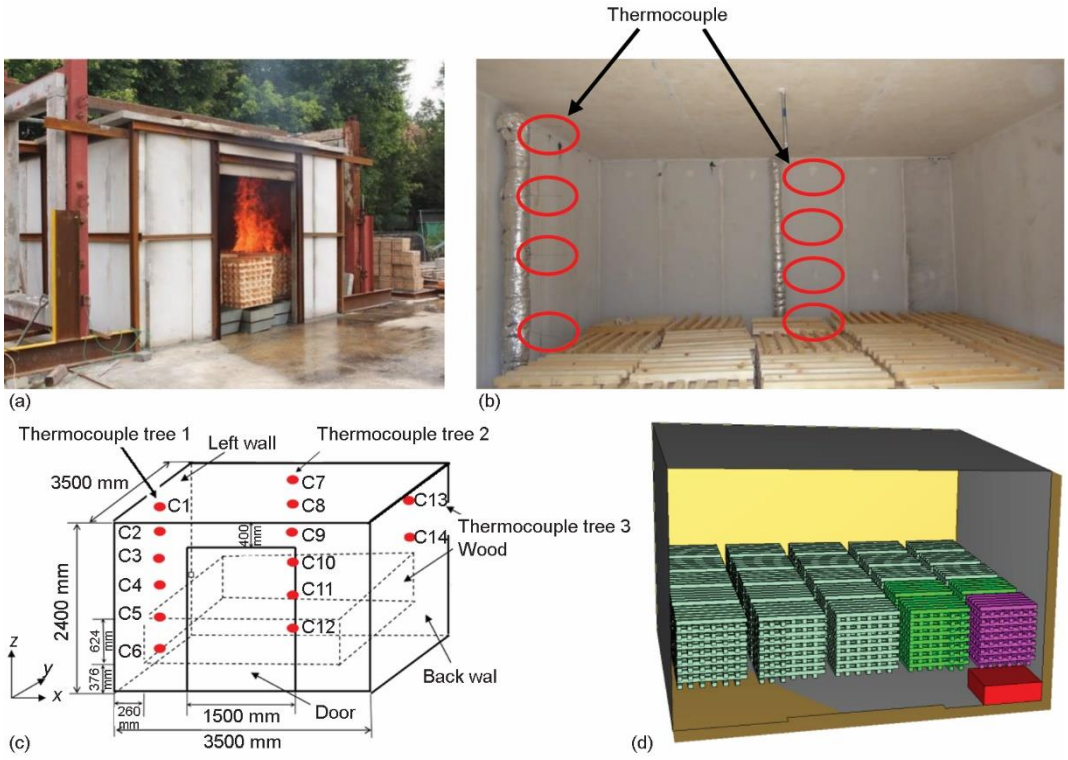

Figure 1. Room geometry; (a) experiment, (b) thermocouples, (c) FDS input, and (d) FDS model

As shown in figs. 1(b) and 1(c), three sets of a total of fourteen thermocouples were placed near the centerline of two side walls. Two sets of thermocouples C1 to C6 and C7 to C12 were placed near the left wall and the back wall, respectively. The uppermost thermocouples C1 and C7 were placed at 2.2 m above the ground, the other thermocouples C2-C6, and C8-C12 were placed at 2, 1.6, 1.2, 0.8, and 0.4 m above the ground, respectively. Two thermocouples

C13 and C14 were placed near the right wall at 2.4 m and 1.6 m above the ground, respectively. During the experiment, the ambient temperature was 20 °C.

Numerical simulations

The FDS was used to predict the temperatures and gas products in a wood fire in this paper. Free boundary conditions were imposed on the computing domains between the fire room and the external environment, which means natural ventilation by door opening. Pressure was taken as the ambient pressure.

Numerical experiments on wood combustion were carried out in a room with geometry shown in fig. 1. The room geometry was the same as in the experiment.

To study the influence of the moisture, computational domain, grid resolution, and the sub-grid scale model coefficient, a total of 19 scenarios were studied, and the computing details are shown in tabs. 1 and 2. Note that the conditions for scenario G3 and W2 are the same. That is just to make it more obvious what the conditions are in each set.

Table 1. Conditions for the simulation scenarios

Scenario	Fuel	Computational domain			Grid size [m]	Total number of cells
		X [m]	*Y* [m]	*Z* [m]		
G1	wood of 15% moisture content	5.3	5.3	3.6	0.06	419050
G2					0.05	808992
G3					0.04	1487200
W1	wood of 15% moisture content	3.5	3.5	2.4	0.04	337014
W2		5.3	5.3	3.6	0.04	1487200
W3		7	7	4.8	0.04	2603952
W2a	wood of 10% moisture content	5.3	5.3	3.6	0.04	1487200
W2b	wood of 5% moisture content					

Using the pyrolysis model in FDS, the wood crib was allowed to burn by itself in the simulations. Considering the safety factor, the water mist system was activated at 3000 seconds in the experiment. Thus, only the data in the first 3000 seconds were considered in this study.

Table 2. Summary of numerical details

Scenario	Input parameter			Scenario	Input parameter		
	C_s	Pr	Sc		C_s	Pr	Sc
1	0.1	0.5	0.5	7	0.2	0.7	0.5
2	0.15	0.5	0.5	8	0.2	0.9	0.5
3	0.2	0.5	0.5	9	0.2	0.5	0.2
4	0.25	0.5	0.5	10	0.2	0.5	0.4
5	0.2	0.2	0.5	11	0.2	0.5	0.7
6	0.2	0.4	0.5	12	0.2	0.5	0.9

The physical properties of the wood were taken as of density 460 kg/m^3, thermal conductivity 0.1 W/mK, and specific heat capacity 1.7 kJ/kgK [26]. The material of the wall in the fire experiment was concrete, with a thermal conductivity of 1.6 W/mK, density of 2400 kg/m^3, and specific heat capacity of 0.92 kJ/kgK. For initial conditions, velocity components, energy and reaction progress variable were set to zero everywhere. The environment temperature and the initial temperature of the inside walls were all 20 °C.

The time step was determined by the Courant-Friedrichs-Lewy (CFL) condition to satisfy the stability criteria [1]. Navier-Stokes equations were used to compute the large eddies, and Smagorinsky sub-grid scale (SGS) model was used to compute the small eddies in all the simulation experiments.

Radiation was computed by a finite volume method combined with a gray gas approach, which is the default model of FDS. The absorption coefficients were computed using RADCAL.

The CFD predicted results were to be compared with experimental data for determining key parameters in the FDS simulations. Further research to justify the CFD results should be proceeded as raised in a recent presentation on CFD fire simulations [27].

Grid sensitivity analysis

Considering the size of a single wood crib, three different scenarios G1-G3 of uniform mesh distribution were tested on the grids. The grids have different sizes of 0.06, 0.05, and 0.04 m, while the total number of grid cells is 419050, 808992, and 1487200, respectively, as shown in tab. 1. Figure 2 shows the grid test results by using different grid systems. Functional analysis results of the point-to-point comparison are also presented in fig. 2. Norms and cosines were calculated for temperature for each grid cell.

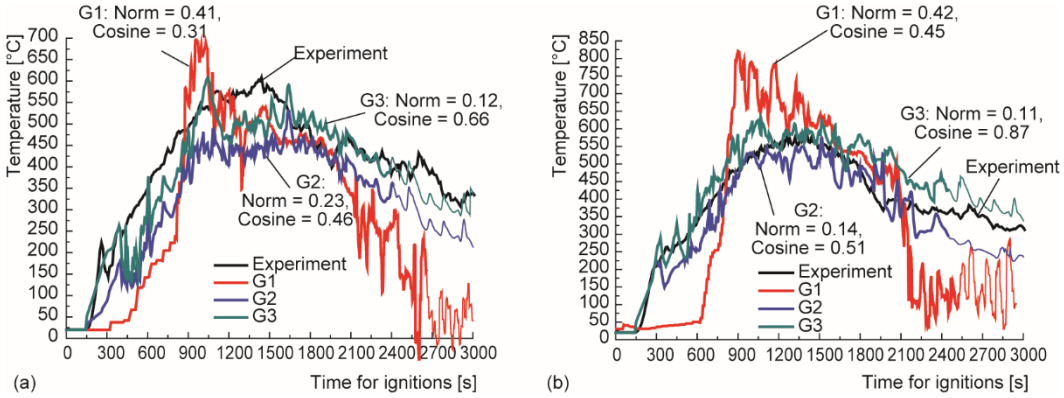

Figure 2. Grid sensitivity; (a) C3 and (b) C9 (*for color image see journal web site*)

It can be observed that the curve derived from the grid resolution of G1 has a similar shape as that of the G2 and G3, however, there were significant fluctuations in this case. Repeated experiments on G1 were carried out, and the fluctuations still existed. The curves derived from grid resolution of G2 and G3 have identical shapes. But it is still necessary to verify that these values are in accordance with the measured ones. In this regard, if experimental measurements and predicted temperature values are compared, the same tendency can be observed, but the values significantly differ for the grid resolutions G2.

The norms of G3 are 0.12 and 011. Among the norm values, the values of G3 are closer to 0. The cosine of G3 are 0.66 and 0.87, which are closer to 1 than G1 and G2.

Though the simulated values of G3 differed from the experimental results at some points, the overall predicted trends of temperature were identical as that of the experiment. Therefore, the grid system of G3 of a grid size of 0.04 m will be used to evaluate the fire model in wood combustion.

Computing domain

In CFD simulations, extending the computing domain outside the fire room was proposed [17, 28] to obtain a better description of free boundaries. Thus, three computing domains labeled as W1-W3 were used, as shown in fig. 3.

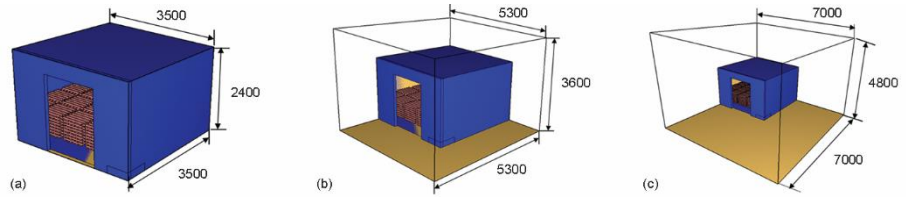

Figure 3. Scenarios W1-W3 [mm]; (a) W1, (b) W2, and (c) W3 (*for color image see journal web site*)

From fig. 4, the temperature using the computing domain W1 has a relatively large deviation from the experiment. Although the results from W3 are closer to the experimental value than W2, the differences are less than 5%.

The norms of W2 are 0.12 and 011, and the norms of W3 are both 0.09. The cosine of W2 are 0.66 and 087, and the norms of W3 are 0.72 and 0.89. They are pretty close. Considering the computer computation time, the computing domain of W2 is adopted in this study.

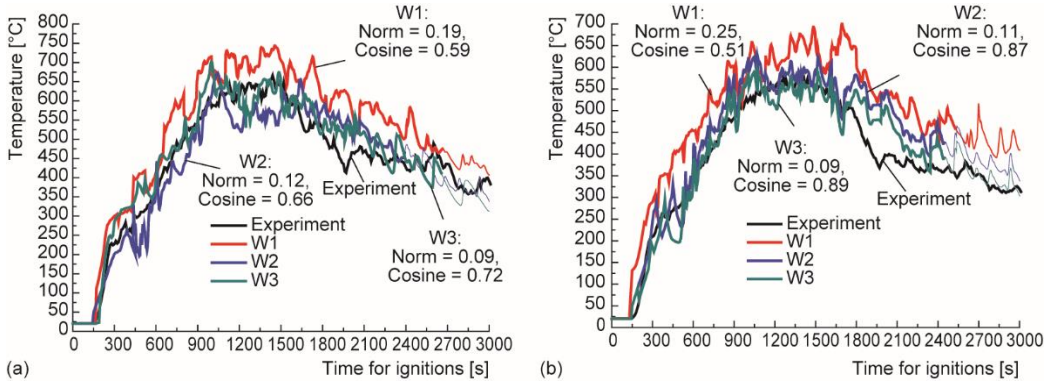

Figure 4. Effect of varying the computing domain; (a) C3 and (b) C9 (*for color image see journal web site*)

Moisture content functional

Changes in moisture content will affect the pyrolysis process greatly and thus affect the predicted temperature. The moisture content of dried wood is usually from 5-15% [29]. Therefore, three moisture contents of 15%, 10%, and 5% were used to investigate the effect of moisture content of the wood used. The conditions are listed in tab. 1.

As shown in fig. 5, the norms of 15% moisture are both 0.14. The cosine of 15% moisture are 0.92 and 086. Among the norm values, the values of 15% moisture are closer to

0. Among the cosine values, the values of 15% moisture are closer to 1. So, the moisture content of the wood used in the experiment might be around 15%. Thus, 15% moisture content will be used in latter discussion.

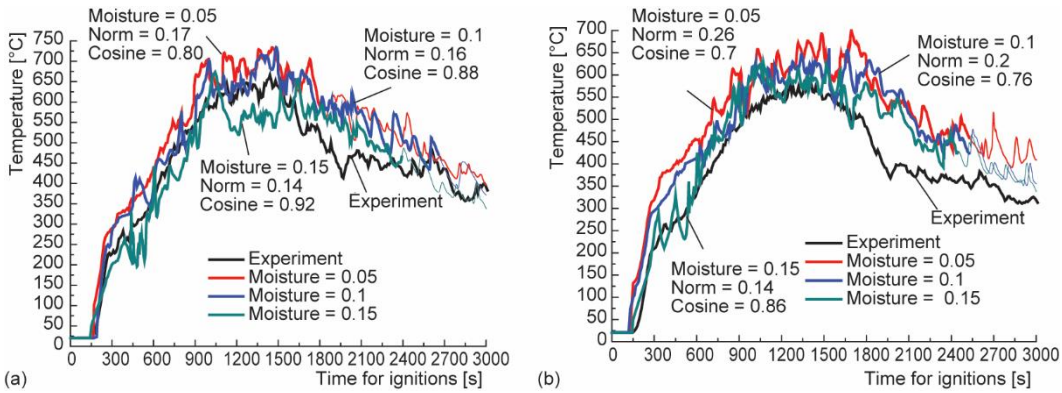

Figure 5. Effect of moisture content; (a) C3 and (b) C9 (*for color image see journal web site*)

Gaseous phase sensitivity analysis

The sensitivity of LES parameters are presented in the following text.

Smagorinsky constant, C_s

The Smagorinsky constant, C_s, has been optimized over a range from 0.1 to 0.25 for various flow fields [30]. For example, C_s is 0.1 for channel flow [31], 0.16 for indoor air-flow [1], and ranges from 0.17 to 0.19 [32] for isotropic turbulent flow. However, it has not been described for the product smoke flow from the burning of wood. In order to study the effect of C_s on wood combustion, the simulation temperature with four bounding values from an empirical correlation (C_s = 0.1, 0.15, 0.2, and 0.25) corresponding to the Scenarios 1-4 will be compared with experimental results, as shown in tab. 2.

From figs. 6 and 7, it can be seen that the predicted temperatures of the point C3 are closer to the experimental data with increasing value of Smagorinsky constant. Large temperature fluctuations occurred when C_s = 0.1. The FDS predictions using C_s of 0.15 and 0.25 show

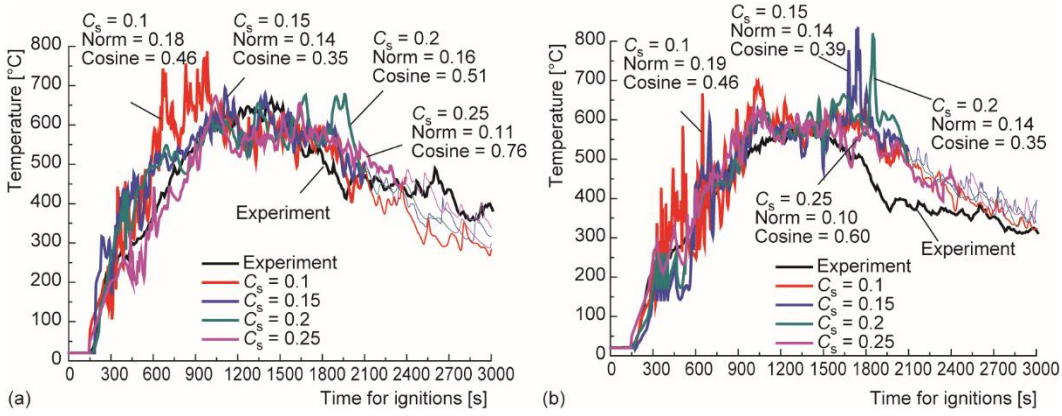

Figure 6. Comparison of predicted temperatures with experimental data at measuring points C3 and C9 - varying the Smagorinsky constant; (a) C3 and (b) C9 (*for color image see journal web site*)

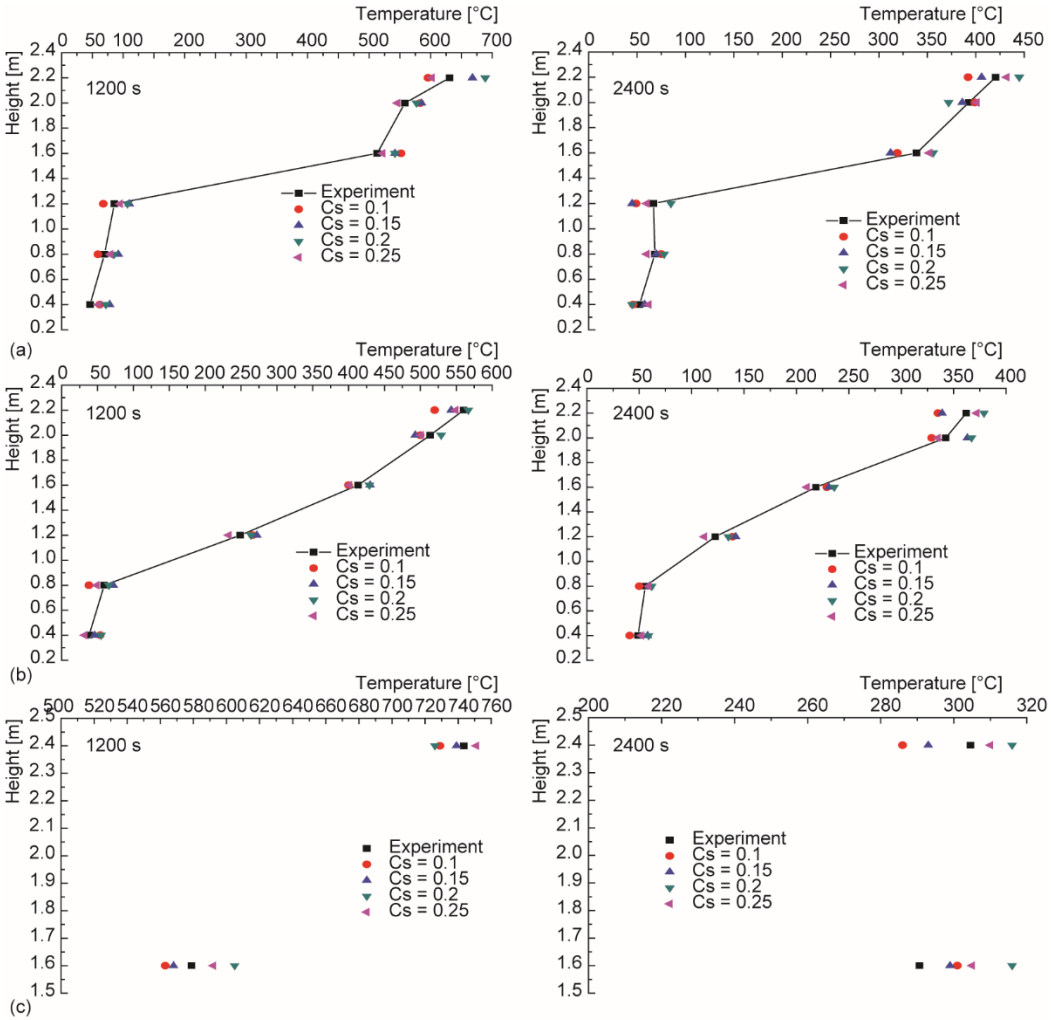

Figure 7. Comparison of predicted temperatures with experimental data at measuring thermocouple trees - varying the Smagorinsky constant; (a) thermocouple tree 1, (b) thermocouple tree 2, and (c) thermocouple tree 3 (*for color image see journal web site*)

a good agreement with the experimental data for point C3 away from the doorway. At point C9 near the doorway, the predicted temperatures show a good agreement with the experimental data in the increasing phase, which are larger than the experimental value in the declining phase. The reason may be that the computational domain is relatively small, and the heat is not easy to disperse from the door in the numerical simulation, which leads to a relatively high temperature compared with the experimental value. From fig. 7, it also can be seen that the SGS model shows some weakness to predict the temperature in the near ceiling region.

When the values of 0.1 and 0.15 are used, the temperatures obtained at the early phase of the simulation at point C9 have larger deviations. Based on these results, a relatively high value of Smagorinsky constant would be appropriate for combustion of wood cribs. When a relatively high value of C_s (0.2) is used, the temperature is overestimated by about 8% compared to the value (0.25).

As shown in fig. 6, when a relatively high value of C_s (0.25) is used, norms are closer to zero and cosines are closer to 1.

It is thus concluded that the value C_s of 0.25 is applicable for wood combustion applications. Although it is presumed that the default value (C_s = 0.2) is applicable for most applications, it is worth to investigate to find out more suitable model coefficient for each fire scenario, especially when highly nonlinear turbulence chemistry interaction involved.

Prandtl number

In order to study the effect of Prandtl number on wood combustion, five values from an empirical correlation, Prandtl number of 0.2, 0.4, 0.5, 0.7, and 0.9 corresponding to scenarios 3, 5 to 8, will be tested, as shown in tab. 2.

As shown in figs. 8 and 9, there are slight differences between the experimental and predicted temperatures with Prandtl number changing. The temperatures are closer to the experimental data at the point C3 under all different values. But some oscillation values exist when Pr = 0.2, 0.7, and 0.9.

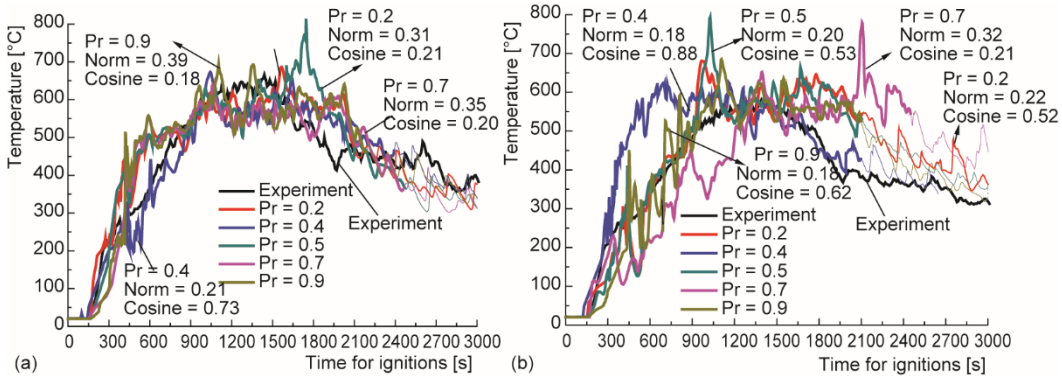

Figure 8. Comparison of predicted temperatures with experimental data at measuring points C3 and C9 - varying the Prandtl number; (a) C3 and (b) C9 (*for color image see journal web site*)

A large discrepancy in temperature is observed at the point C9 due to the longer distance from the door and the heat is difficult to disperse in the simulation. Just like the Smagorinsky constant, temperatures show a good agreement with the experimental data in the increasing phase, which are larger than the experimental value in the declining phase. The discrepancies are within 10% under other values.

As shown in fig. 8, the norms for Pr = 0.4 are closer to zero and cosines are closer to 1.

The predicted values using Pr = 0.4 are closest to the experimental results. Thus, it is concluded that the value of Pr = 0.4 is applicable for wood combustion condition.

Schmidt number

The Schmidt number of 0.2, 0.4, 0.5, 0.7, and 0.9 corresponding to scenarios 3, 9, to 12 are used for the sensitivity analysis for wood combustion in the room, as shown in tab. 2. The default value in FDS is 0.5.

The comparison of temperatures in the analysis is shown in figs. 10 and 11. It is evident that the FDS predictions change little as the Schmidt number is varied. Generally, a Schmidt number of 0.7 gives good results. As shown in fig. 10, the norms for Sc = 0.7 are closer to zero and cosines are closer to 1.

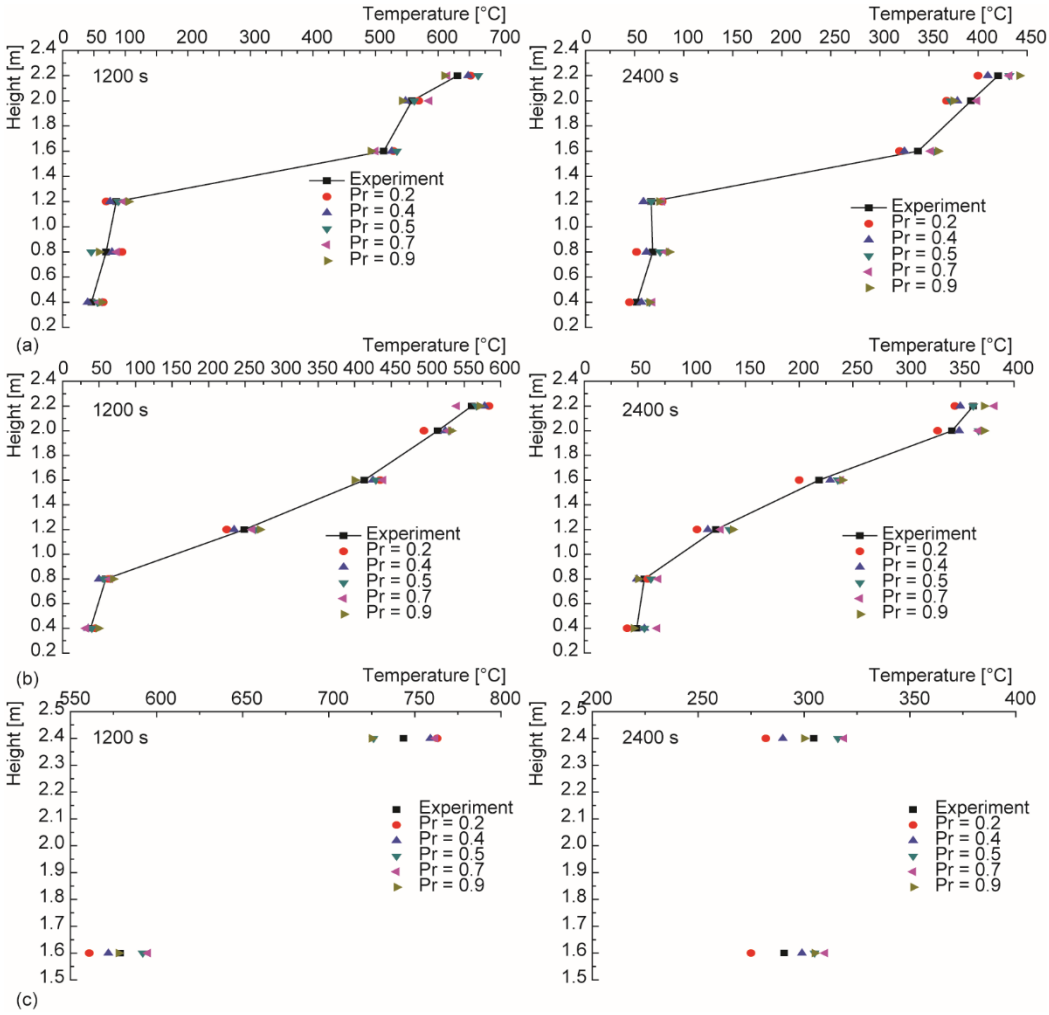

Figure 9. Comparison of predicted temperatures with experimental data at measuring thermocouple trees - varying the Prandtl number; (a) thermocouple tree 1, (b) thermocouple tree 2, and (c) thermocouple tree 3 (*for color image see journal web site*)

Flammability diagram

For the fire safety control of wood structure, in addition to improving the accuracy of numerical simulation method, we also need to find ways to reduce the probability of fire outbreak. Therefore, the flammability limits of wood are particularly important.

If gas mixture is exposed to heat or an ignition source, and the concentration of the mixture is within the flammability range, a fire may result. Since a gas mixture of a flammable gas and an oxidant can be ignited only if the concentration of the flammable gas lies within a given range known as the flammability limits, the data of flammability limits are crucial to developing safe practices for handling flammable gases.

Wood-based materials are widely used for structural and non-structural applications today. For this reason, studies on flammability limits of wood are valuable works. Accurate

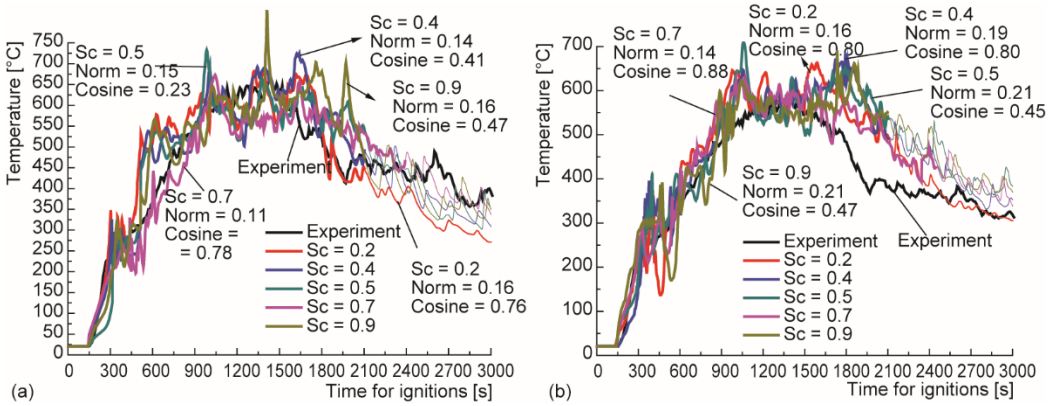

Figure 10. Comparison of predicted temperatures with experimental data at measuring points C3 and C9 - varying the Schmidt number; (a) C3 and (b) C9 (*for color image see journal web site*)

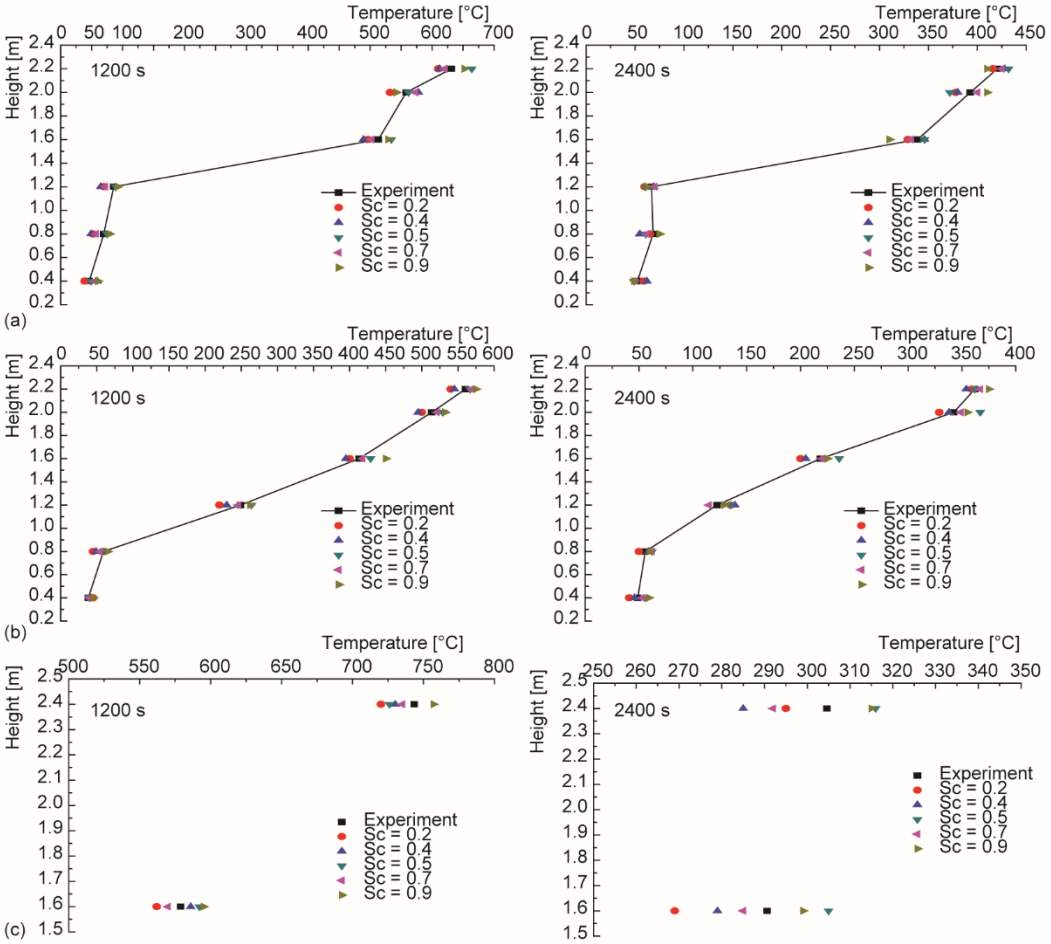

Figure 11. Comparison of predicted temperatures with experimental data at measuring thermocouple trees - varying the Schmidt number; (a) thermocouple tree 1, (b) thermocouple tree 2, and (c) thermocouple tree 3 (*for color image see journal web site*)

information on flammability limit is necessary for safe handling of flammable or combustible gas in the industry. Prevention of unwanted fire accidents requires the knowledge of flammability characteristics [33].

In the flammability diagram, the fire triangle indicates the three essential elements to ignite ordinary burning and fires: fuel, oxygen and heat. A mixture is flammable only when its composition is between the lower flammability limit (LFL) and the upper flammable limit (UFL). The LFL identifies the smallest mixture able to sustain a flame. The UFL identifies the richest flammable mixture. The flammable range is the range of a gas concentration that will burn if an ignition source is introduced. Below the flammable range, the mixture is too lean to burn, and above the upper flammable limit, the mixture is too rich to burn. These flammability limits can be measured experimentally and by a theoretical approach.

Equations (11) and (12) are the ways to predict flammable limits LFL and UFL for hydrocarbons [34]:

$$\mathrm{LEL} = 0.55\, C_{\mathrm{st}} \tag{11}$$

$$\mathrm{UEL} = 3.5\, C_{\mathrm{st}} \tag{12}$$

where 0.55 and 3.5 are constants and C_{st} is the stoichiometric concentration which can be expressed as eq. (13), fuel in mixture [vol.%].

$$C_{\mathrm{st}} = \frac{21}{0.21 + n} \tag{13}$$

where n is the number of moles of O_2 required for complete combustion of one mole of fuel by the reaction eq. (1).

Assume that the wood has been degraded into a gaseous fuel. The volatile gases are instantaneously transported to the surface. Assume the wood does not contain moisture.

According to the combustion reaction eq. (1), n is 3.7 with the corresponding C_{st} of 5.37, so the LFL and UFL of $C_{3.4}H_{6.2}O_{2.5}$ at ambient pressure and temperature of theoretical values are 2.95 vol.% and 18.80 vol.%, respectively. The coefficients of 21 and 0.21 are based upon the O_2 concentration in air.

Another important parameter to prevent fire is the limiting oxygen concentration (LOC), which is defined as the minimum oxygen concentration in a mixture of fuel, air and inert gas:

$$\mathrm{LOC} = \mathrm{z}\, LFL = 3.7 \times 2.95\% = 10.92\% \tag{14}$$

The intersection of the stoichiometric line with the oxygen axis (in vol.% oxygen) is given by:

$$100\frac{z}{z+1} = 100\frac{3.7}{3.7+1} = 78.72\% \tag{15}$$

From Chen [35], the value of the volume fraction of the flammability limit in pure oxygen is:

$$\mathrm{UFL}_{\mathrm{O}_2} = \frac{\mathrm{UFL}_{\mathrm{air}} Cp_{\mathrm{f}} + 0.79(1 - \mathrm{UFL}_{\mathrm{air}}) Cp_{\mathrm{N}_2}}{0.79\mathrm{UFL}_{\mathrm{air}}(Cp_{\mathrm{f}} - Cp_{\mathrm{N}_2}) + (0.21 Cp_{\mathrm{f}} + 0.79 Cp_{\mathrm{N}_2})} = \frac{0.188 \times 1200 + 0.79(1 - 0.188)1.038}{0.79 \times 0.188(1200 - 1.038) + (0.21 \times 1200 + 0.79 \times 1.038)} = 52.51\% \tag{16}$$

$$\mathrm{LFL}_{\mathrm{O}_2} = \frac{\mathrm{LFL}_{\mathrm{air}} Cp_{\mathrm{O}_2}}{\mathrm{LFL}_{\mathrm{air}} Cp_{\mathrm{O}_2} + (1-\mathrm{LFL}_{\mathrm{air}})(0.21 Cp_{\mathrm{O}_2} + 0.79 Cp_{\mathrm{N}_2})} = \\ = \frac{0.0295 \times 0.909}{0.0295 \times 0.909 + (1-0.0295)(0.21 \times 0.909 + 0.79 \times 1.038)} = 2.66\% \tag{17}$$

The specific heat capacities of wood are the means of estimates, Schaelin *et al.* [28]:

$$Cp_{\mathrm{f}} = 1.2 \cdot 10^3 \text{ J/kg°C}, \quad Cp_{\mathrm{O}_2} = 0.909 \text{ J/kg°C}, \quad Cp_{\mathrm{N}_2} = 1.038 \text{ J/kg°C}$$

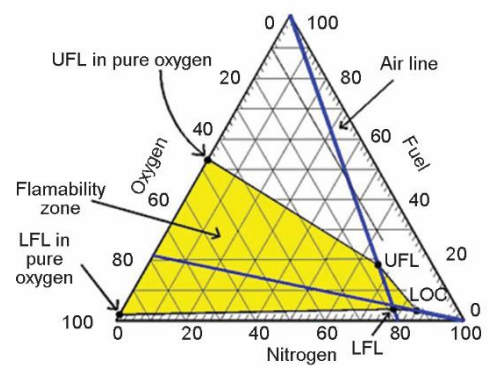

Figure 12. Flammability diagram for wood

The standard flammability diagram for wood is redrawn as in fig. 12. The use of triangular co-ordinates like fig. 12 makes the examination of a three-component system easier because all three constants are presented on the graph at one time. The flammability diagram of fuel, O_2, and N_2 mixture represents the three components, respectively, and the areas encompassed by overlapping sets of oblique lines are the flammable zones for the wood.

Conclusions

The purpose of this paper is to assess combustion simulations by FDS with selected common fuels based on experiment, and to investigate how the model can be applied in fire engineering approach. The effects of different grid systems, computing domains and moisture contents on the predictions were studied first, which were then used to study the gaseous phase sensitivity.

The sensitivity of the parameters Smagorinsky constant, turbulent Schmidt number, and turbulent Prandtl number were discussed for a more accurate assessment of the solid combustion characteristics using FDS. The predictions for temperature agreed reasonably well with the experiment with the values of 0.25 for Smagorinsky constant, 0.7 for turbulent Schmidt number, and 0.4 for turbulent Prandtl number.

The hazard of the generation of fire products in chemical reactions is a vital factor for assessing fire risk and fire protection. Theoretical results of mass fractions of species for the wood were obtained using the parameter of equivalence ratio.

The flammability diagram of wood was obtained. Based on the standard flammability diagram for studying combustion, the flammability envelope and the critical mass fraction of the volatilized unburnt fuel can be obtained directly. The flammability diagram consists of three axes representing the mass fractions of unburnt fuel (assume that the wood has been degraded into a gaseous fuel), oxygen and nitrogen. The moisture content of wood and the products of the combustion process are not included.

The research of this subject has important reference value and guiding significance for the fire safety and fire warning of wooden building. Though the simulated values differed from the experimental results at some points, the overall predicted trends of temperature were identical as that of the experiment.

Acknowledgment

The work described in this paper was partially supported by Research Grants Council of the Hong Kong Special Administrative Region, China for the project *A study on powder explosion hazards and control schemes when clouds of coloured powder are sprayed in partially confined areas* (Project No. PolyU 15252816) with account number B-Q53X, and partially supported by the Fundamental Research Funds for the Central Universities (Grant No. 2019JBM087) and Natural Science Foundation of China (Grant No. 52072027) with funding granted to Dr Y. H. Xi.

Nomenclature

A – pre-exponetial factor, or frequency factor, [s^{-1}]
Cp – specific heat capacity, [$Jkg^{-1}K^{-1}$]
C_s – Smagorinsky constant
C_{st} – stoichiometric concentration
E – activation energy, [$kJmol^{-1}$]
k – reaction rate constant, [s^{-1}]
n – number of moles
Pr – Prandtl number
R – universal gas constant, 8.314×10^{-3} KJ/molK
Sc – Schmidt number
T – reaction temperature, [K]

References

[1] Chow, W. K., Experience on Implementing Performance-Based Design in Hong Kong, *Proceedings*, 9thAsia-Oceania Symposium on Fire Science and Technology, 2012, Hefei, China
[2] Chow, W. K., Fire Safety Concerns for Subway Systems in Hong Kong, *Proceedings*, Fire Safety Asia Conference (FiSAC) 2011, Suntec, Singapore
[3] Cox, G., Kumar, S., Modelling Enclosure Fires using CFD, in: *SFPE Handbook of Fire Protection Engineering*, 3rd Edition, Quincy, Mass., USA, pp. 3-194–3–218, 2002
[4] Chow, C. L., Chow, W. K., A Brief Review on Applying Computational Fluid Dynamics in Building Fire Hazard Assessment, in: *Fire Safety* (Eds. I. Søgaard and H. Krogh), Nova Science Publishers, N. Y., USA, 2009
[5] Chow, W. K., *et al.*, Numerical Studies on Atrium Smoke Movement and Control with Validation by Field Tests, *Building and Environment*, *44* (2009), 6, pp. 1150-1155
[6] Cai, N., Chow, W. K., Numerical Studies on Heat Release Rate in a Room Fire Burning Wood and Liquid Fuel, *Building Simulation - An International Journal*, *7* (2017), 5, pp. 511-524
[7] Harper, C. A., *Handbook of Building Materials for Fire Protection*, McGraw-Hill, N. Y., USA, 2004
[8] Horasan, M., Fire safety challenges, *Proceedings*, International Fire Conference & Exhibition Malaysia, Kuala Lumpur Convention Center, Malaysia, 2012
[9] Uddin, M., Kiviranta. K., Casein-Magnesium Composite as an Intumescent Fire Retardant Coating for Wood, *Fire Safety Journal*, *112* (2020), Mar., ID 102943
[10] Song, K., Ganguly, I., High Temperature and Fire Behavior of Hydrothermally Modified Wood Impregnated with Carbon Nanomaterials, *Journal of Hazardous Materials*, *384* (2020), Feb., ID 121283
[11] Diab, M. T., *et al.*, The Behaviour of Wood Crib Fires under Free Burning and Fire Whirl Conditions, *Fire safety Journal*, *112* (2020), Mar., ID 102941
[12] Kalali, E. N., *et al.*, Flame-Retardant Wood Polymer Composites (WPCs) as Potential Fire Safe Bio-Based Materials for Building Products: Preparation, Flammability and Mechanical Properties, *Fire Safety Journal*, *107* (2017), July, pp. 210-216
[13] Janicka, J., Sadiki, A., Large Eddy Simulation of Turbulent Combustion Systems, *Proceedings of the Combustion Institute*, *30* (2005), 1, pp. 537-547
[14] Pope, S., *Turbulent Flows*, Cambridge University Press, Cambridge, Mass., USA, 2000
[15] McGrattan, K., Recent Developments in FDS and CFAST, *Proceedings*, SFPE North America Conference & Expo, Montreal, Canada, 2017
[16] Ritchie, S. J., *et al.*, Effect of Sample Size on the Heat Release Rate of Charring Materials, *Proceedings*, 5th International Symposium on Fire Safety Science (ed. Y. Hasemi), Boston, Mass., USA, 1997, pp. 177-188
[17] Cai, N., Chow, W. K., Numerical Studies on Heat Release Rate in Room Fire on Liquid Fuel under Different Ventilation Factors, *International Journal of Chemical Engineering*, *2012* (2012), ID 910869

[18] Li, X., *et al.*, Combustion Behaviors and Characteristic Parameters Determination of Sassafras Wood under Different Heating Conditions, *Energy*, *203* (2020), July, ID 117831
[19] Atreya, A., Pyrolysis, Ignition and Fire Spread on Horizontal Surfaces of Wood, National Bureau of Standards, Gaithersburg, Md., USA, Report NBS-GCR-83-449, 1984
[20] McGrattan, K., *et al.*, NIST Special Publication 1019 Sixth Edition Fire Dynamics Simulator User's Guide, National Institute of Standards and Technology, Gaithersburg, Md., USA, 2020
[21] Chow, W. K., *et al.*, News from The Hong Kong Polytechnic University, *International Association for Fire Safety Science Newsletter* (ed. G. Rein), *34* (2013), pp. 12-13
[22] Starink, M. A New Method for the Derivation of Activation Energies from Experiments Performed at Constant Heating Rate, *Thermochim Acta*, *288* (1996), 1-2, pp. 97-104
[23] Peacock, R. D., *et al.*, Quantifying Fire Model Evaluation Using Functional Analysis, *Fire Safety Journal*, *33* (1999), 10, pp. 167-184
[24] Chow, W. K., Zou, G. W., Numerical Simulation of Pressure Changes in Closed Chamber Fires, *Building Environment*, *44* (2009), 6, pp. 1261-1275
[25] Chow, W. K., *et al.*, Simulating Smoke Filling in Big Halls by Computational Fluid Dynamics, *Modelling and Simulation in Engineering*, *2011* (2011), ID 781252
[26] Matala, A., Estimation of Solid Phase Reaction Parameters for Fire Simulation, M. Sc. thesis, Helsinki University of Technology, Helsinki, Finland, 2008
[27] Fan, W. C., *et al.*, Advancement of Computational Heat Transfer in Fire Research in China, *Proceedings*, ASME 2013 Heat Transfer Summer Conference, Minneapolis, Minn., USA, Paper no. HT2013-17409, 2013
[28] Schaelin, A., *et al.*, Simulation of Airflow through Large Openings in Buildings, *Proceedings*, ASHRAE Winter Meeting, Anaheim, Cal., USA, 1992, pp. 319-328
[29] Ragland, K. W., *et al.*, Properties of Wood for Combustion Analysis, *Bioresource Technology*, *37* (1991), 2, pp. 161-168
[30] Zhang, W., *et al.*, Turbulence Statistics in a Fire Room Model by Large Eddy Simulation, *Fire Safety Journal*, *37* (2002), 8, pp.721-752
[31] Quintiere, J., *et al.*, Wall Flames and Implications for Upward Flame Spread, *Combustion Science and Technology*, *48* (1985), 3-4, pp. 191-222
[32] Kwon, J., Evaluation of FDS V.4: Upward Flame Spread, M. Sc. thesis, Worcester Polytechnic Institute, Worcester. Mass., USA, 2006
[33] Madrzykowski, D., Stroup, D. W., Flammability Hazard of Materials, in:, *Fire Protection Handbook* (eds. A. E. Cote, *et al.*), 20th Edition, National Fire Protection Association, Quincy, Mass., USA, 2008, Volume 1, Chapter 3, Section 2, pp. 2/31-48
[34] Liu, B., Recommended Calculation of Explosion Limitation for Organic Burning Gas (in Chinese), *Journal of Kunming University of Science and Technology (Science and Technology)*, *32* (2007), 1, pp. 119-124
[35] Chen, C. C., A Study on Estimating Flammability Limits in Oxygen, *Industrial & Engineering Chemistry Research*, *50* (2011), 17, pp. 10283-10291

Paper submitted: August 18, 2018
Paper revised: August 31, 2020
Paper accepted: September 1, 2020

© 2021 Society of Thermal Engineers of Serbia.
Published by the Vinča Institute of Nuclear Sciences, Belgrade, Serbia.
This is an open access article distributed under the CC BY-NC-ND 4.0 terms and conditions.